

# Tomography Reconstruction Based on Null Space Search

Tibor Lukić and Tamara Kopanja

Faculty of Technical Sciences, University of Novi Sad, Serbia  
tibor@uns.ac.rs, kopanja.v11.2019@uns.ac.rs

**Abstract.** The paper introduces a new tomography reconstruction approach for gray and binary image reconstruction. The proposed method intends to find a solution by searching for the best linear combination of the basis vectors of the null space of the projection matrix. One of the advantages of the proposed approach is that the projection error remains always extremely low, practically equal to zero, during the reconstruction process. The method applies a gradient based optimization algorithm. A short experimental evaluation, including three relevant and well-know algorithms for comparison, is presented.

**Keywords:** Tomography reconstruction · Null space · Energy minimization · Gradient based optimization · Regularization

## 1 Introduction

*Tomography* is a field of image processing which deals with reconstruction of unknown images from available projection data [7]. Mathematically, the image can be modeled by a function whose codomain or range may be continuous or discrete set. In the *Computerized Tomography* the image function has a continuous range. The *Discrete Tomography* (DT) [8, 9] is a sub-field of tomography, where the range of the image function is a finite and discrete set. If this range contains just a few predefined intensity levels, then we talk about *Multi-Level Tomography* [12]. In particular, in *Binary Tomography* (BT), the unknown image contains only two different intensity values, usually zero and one.

Application spectrum for tomography methods is very wide. Tomography image reconstruction techniques are widely used in different industrial investigation problems, often in the form of nondestructive material testing [4]. Another vast field of its application is connected to the human radiology diagnostic procedures, like CT scanning. Great field of tomography application belongs to security screening techniques, for example, many airports use X-rays computed tomography for screening baggage [11]. BT methods are extremely useful in cases when we investigate the presence or absence of a specific material inside a homogeneous structure, for example in the determination of the presence of atoms in crystalline structures [10].

There are several successful methods, proposed in literature, for solving the tomography reconstruction problem. We just mention a few well-known iterative algorithms: *Algebraic Reconstruction Technique* (ART) [6], *Simultaneous*

*Iterative Reconstruction Technique* (SIRT) [5], *Discrete Algebraic Reconstruction Technique* (DART) [2, 1], *Spectral Projected Gradient* (SPG) [15], *Difference of Convex functions* (DC) [21]. The common feature of these methods is that they change the pixel intensities of the current solution in attempt to reduce the projection error, in other words, the projection error is minimized by the convergence process of these methods. As a result of that, the projection error may be minimized with smaller or higher success. This issue motivated us to develop a reconstruction method where the projection error does not change during the iterative process.

In the reconstruction process the basic criteria is the matching of the reconstructed image with the measured projection data. The acquired data is often the most reliable information about the unknown image. Therefore, it is important that the projection error of the reconstructed image remains as small as possible. In this paper we propose a new reconstruction method which seeks to answer to this issue. In the proposed reconstruction process the projection error always remains unchanged and theoretically equals to zero - in practical applications close to zero.

The paper has the following structure. Section 2 gives the description of the basic tomography reconstruction problem. In Section 3 the new reconstruction method is presented. In Section 4 a short experimental evaluation of the proposed new reconstruction method is given. Finally, the conclusion is given in the Section 5.

## 2 Tomography reconstruction problem

In this paper we consider transmission tomography reconstruction model. The main characteristic of transmission tomography is that the both, source and detector are placed out of the considered object. Mathematically the problem of tomography reconstruction may be formulated by the following system of linear equations

$$A u = b, \quad A \in \mathbb{R}^{m \times n}, \quad u \in \mathbb{R}^n, \quad b \in \mathbb{R}^m, \quad (1)$$

where  $u$  represents the unknown image which should be reconstructed. In the case of binary tomography, components of vector  $u$  have only two different values, usually 0 and 1. The matrix  $A$  is so-called *projection matrix* and its rows hold information about a length of the projection ray passing through the pixel. The assumption is that each pixel is represented as a square with unit side length, see Fig. 1. Further, it represents calculation projection value for a given image from one projection direction denoted by angle  $\theta$ . The another projection direction is obtained by rotation source-detector system around of the center of the circle. Each projection direction contributes a new parallel set of the projection rays. Detected projection values are placed in the projection vector  $b$ . It is not hard to see that the projection matrix  $A$  is sparse, i.e. the majority of elements  $a_{i,j}$  are equal to zero.

In the reconstruction problem, both the matrix  $A$  and the projection vector  $b$  are given, as a calculated or measured data. The task is to determine the

unknown image  $u$ . The system (1) is often underdetermined ( $m \ll n$ ), and consequently, in general case, we can count on an infinite number of possible solutions. The applied parallel beam projection geometry, see Fig. 1, allows us to assume that the matrix  $A$  is full row rank, that is  $\text{rank}(A) = m$ . Therefore, the general solution has  $n - m$  degrees of freedom.

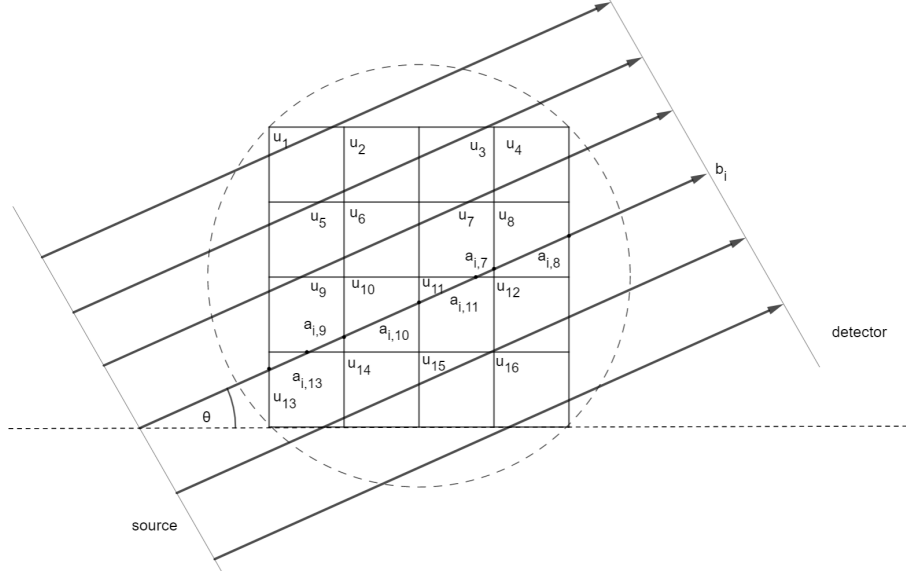


Fig. 1: The transmission parallel beam projection geometry. The  $i$ -th projection value is obtained as  $b_i = a_{i,13}u_{13} + a_{i,9}u_9 + a_{i,10}u_{10} + a_{i,11}u_{11} + a_{i,7}u_7 + a_{i,8}u_8$ .

### 3 Tomography reconstruction method based on null space search

In this section we introduce a new tomography reconstruction method for both gray-scale and binary image reconstructions. The main idea uses the fact that any solution of the projection linear system of equations (1)

$$A u = b,$$

can be represented as a sum of one particular solution  $u_p$  ( $A u_p = b$ ) and an appropriate vector belongs to the null space of the matrix  $A$ , defined by

$$\mathcal{N}(A) = \{x \in \mathbb{R}^n \mid A x = 0\}.$$

Hence the set of all solutions can be represented as

$$u_p + z, \text{ where } z \in \mathcal{N}(A).$$

Let us denote a basis of the vector space  $\mathcal{N}(A)$  by the set of vectors  $\{\mathbf{b}_1, \mathbf{b}_2, \dots, \mathbf{b}_k\}$ , where  $k = n - m$ . Each solution of the system (1) may be represented in the following form

$$w(\alpha) = u_p + \alpha_1 \mathbf{b}_1 + \alpha_2 \mathbf{b}_2 + \dots + \alpha_k \mathbf{b}_k, \quad (2)$$

where  $\alpha = (\alpha_1, \alpha_2, \dots, \alpha_k) \in \mathbb{R}^k$  and  $\mathbf{b}_i \in \mathbb{R}^n$  for all  $i = 1, \dots, k$ .

Now we will choose coefficients  $\alpha_1, \alpha_2, \dots, \alpha_k$  in  $\alpha$  in a such way that the obtained solution  $w(\alpha) \in \mathbb{R}^n$  lies in a predefined area, for example in the hyper cube  $[0, 1]^n$ . To achieve this, let us look at the following unconstrained optimization problem

$$\arg \min_{\alpha} \sum_{i=1}^n W(w(\alpha)_i), \quad (3)$$

where  $W$  is a specially designed potential function. It is defined by

$$W(x) = \begin{cases} x^2, & x \leq 0 \\ (x-1)^2, & x \geq 1 \\ 0, & 0 < x < 1 \end{cases}. \quad (4)$$

$W$  is a continuously differentiable function consisting of two square parabolas and a horizontal line. Its important property is that it is always greater than zero except for values between 0 and 1, when it is zero, see Fig. 2. Therefore, the solution  $\alpha^*$  of the problem (3) gives a combination of coefficients of basis vectors in (2) for which the corresponding image solution  $w(\alpha^*)$  belongs to the set  $[0, 1]^n$ .

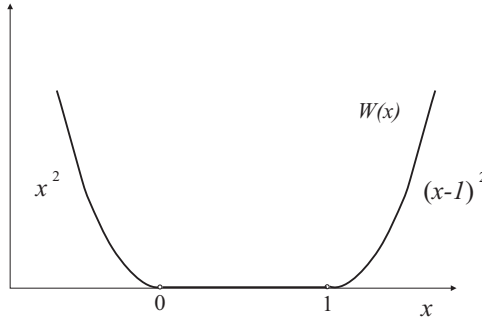


Fig. 2: Potential function  $W$ , designed for reconstruction of gray solution that belongs to the hyper cube  $[0, 1]^n$ .

The gradient of the objective function  $G(\alpha) := \sum_{i=1}^n W(w(\alpha)_i)$  in the optimization problem (3) can be determined by elementary calculus and in analytical way.

It has the following form

$$\text{grad } G(\alpha) = N^T \cdot [W'(w(\alpha)_1), W'(w(\alpha)_2), \dots, W'(w(\alpha)_n)]^T,$$

where the matrix  $N \in \mathbb{R}^{n \times k}$  represents the null space  $\mathcal{N}(A)$  in a way that it contains its basis vectors in the following way

$$N = \begin{bmatrix} b_{11} & b_{12} & \dots & b_{1k} \\ b_{21} & b_{22} & \dots & b_{2k} \\ \vdots & \vdots & \vdots & \vdots \\ b_{n1} & b_{n2} & \dots & b_{nk} \end{bmatrix} = [\mathbf{b}_1 \ \mathbf{b}_2 \ \dots \ \mathbf{b}_k].$$

In practical applications, this matrix can be obtained by elementary calculus, or just by applying the fast Matlab command  $N = \text{null}(A)$ . For the minimization of the problem (3) different gradient type deterministic algorithms can be used. We suggest the Spectral Conjugate Gradient algorithm [3], which shows best performance in our experiments.

It is necessary to determine one solution (a particular solution)  $u_p$  of the system (1), since  $u_p$  is needed in the formula  $w(\alpha)$  (2). We suggest the least norm solution  $u_{LN}$ , for this purpose. The algorithm of the Conjugate Gradient [19] provides a very fast and very accurate calculation of  $u_{LN}$ . Accordingly, the calculation of particular solution in (2) does not reduce the speed and accuracy of the whole reconstruction procedure.

The design of the proposed model (3) is such that the projection error of the solution ( $\|A w(\alpha^*) - b\|$ ) is always extremely low, practically equal to zero. This is achieved by the manner of searching for the solution: the coefficients of basis vectors of the null space (2) are changing during the process, however, this change in the values has no effect on the projection error - this error always remains practically zero. We emphasize that this fact is one of the main advantages of the proposed reconstruction method. The projection data is the most accurate information about the solution in the tomography image reconstruction, hence their accordance with the reconstruction is extremely important. The proposed new method, which we will call *Null Space Search based Tomography* (NSST), has just this feature.

In a case when our goal is to find the binary solution of the tomography reconstruction problem (1), this can be achieved if we replace the potential function (4) in the proposed NSST method with the two well potential function defined by

$$W_2(x) = \begin{cases} x^2, & x \leq v_1 \\ (x-1)^2, & x \geq v_2 \\ h - c(x-p)^2, & v_1 < x < v_2 \end{cases}, \quad (5)$$

where for the given parameter  $l$  we set

$$p = \frac{1}{2}, \quad v_1 = p - l, \quad v_2 = p + l, \quad c = \frac{1}{2l} - 1 \text{ and}$$

$$h = \frac{1}{4}(1 - 2l)$$

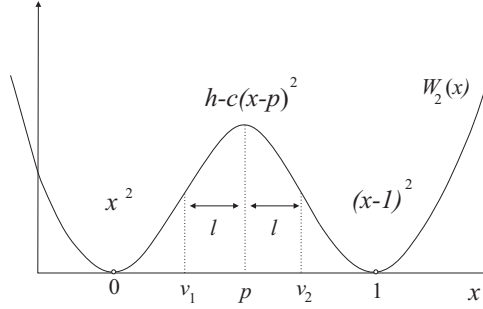


Fig. 3: Potential function  $W_2$  (5), designed for reconstruction of binary solutions.

Function  $W_2$  has 2 minima in the points 0 and 1, such that  $W_2(0) = W_2(1) = 0$ , see Fig. 3. It is a piece-wise quadratic function, where the constants  $h$  and  $c$  are determined in such a way that the function  $W_2$  is continuously-differentiable for each  $x$ . Therefore, the following optimizing problem

$$\arg \min_{\alpha} \sum_{i=1}^n W_2(w(\alpha)_i), \quad (6)$$

can be solved in the same deterministic manner as it is suggested for the model (3) - by a gradient based optimization algorithm.

The solution  $\alpha^*$  of (6) determines a binary image solution  $w(\alpha^*)$  of the tomography problem (1). This means that the proposed reconstruction model (6) defines a variant of the NSST method which belongs to the binary tomography reconstruction methods. The pseudo-algorithm of this method is presented in Alg. 1. The proposed approach envisages reconstruction by the sequence of optimization steps, where the parameter  $l$ , starting from its largest possible value  $\frac{1}{2}$  (for which  $W_2$  reduces to  $W$ ), gradually decreased in each step. This process slowly enforces the "binarization" of the the current solution. The whole process is terminated when the (almost) binary solution is achieved, which is controlled by the exit condition of the *while* loop.

In many proposed tomography reconstruction models, different types of regularization approaches are applied in terms to enhance the quality of reconstructions, see [13, 18, 14]. The quadratic total variation type regularization, which in continuous case has a form

$$\iint_{\Omega} \|\nabla u(x, y)\|^2 dx dy, \quad (8)$$

has an isotropic diffusion type effect on an applied image  $u(x, y)$ , and it is often used in tomography reconstruction [22, 16, 17]. These good experiences motivated us to adapt and add this regularization to the our model as well. Accordingly, we propose the following regularized reconstruction model

$$\arg \min_{\alpha} \sum_{i=1}^n W_2(w(\alpha)_i) + \mu \sum_{i=1}^n (w(\alpha)_i - w(\alpha)_r)^2 + (w(\alpha)_i - w(\alpha)_b)^2, \quad (9)$$

**Algorithm 1:** NSST algorithm for binary reconstruction

---

**Parameters:**  $\epsilon_{out} = 0.1$ ,  $l = \frac{1}{2}$ ,  $l_{\Delta} = 0.001$ ,  $\alpha^{init} = (0, 0, \dots, 0)$ .

**while**  $|w(\alpha^{init})^T \cdot ((1, 1, \dots, 1) - w(\alpha^{init}))| > \epsilon_{out}$   
**do**  
  /\* Solve by SCG algorithm: \*/  

$$\alpha^{new} = \arg \min_{\alpha} \sum_{i=1}^n W_2(w(\alpha)_i) \quad (7)$$
  
   $\alpha^{init} = \alpha^{new}$   
   $l \leftarrow l - l_{\Delta}$   
**end**

---

where indices  $r$  and  $b$  point to neighbour pixels right and below from  $w(\alpha)_i$ , respectively. The parameter  $\mu > 0$  balances between intensity of influence of two different terms in the proposed energy function (9), its value is set to 0.01 in our experiments. Let us denote the second term by  $H(\alpha) = \sum_{i=1}^n (w(\alpha)_i - w(\alpha)_r)^2 + (w(\alpha)_i - w(\alpha)_b)^2$ . This function is an adapted discrete version of the operator (8). The analytical expression of its gradient is given by  $\text{grad } H(\alpha) = \left[ \frac{\partial H(\alpha)}{\partial \alpha_1}, \frac{\partial H(\alpha)}{\partial \alpha_2}, \dots, \frac{\partial H(\alpha)}{\partial \alpha_k} \right]^T$ , where

$$\frac{\partial H(\alpha)}{\partial \alpha_i} = 2 \sum_{l=1}^{l=k} (w(\alpha)_l - w(\alpha)_r)(b_{li} - b_{ri}) + (w(\alpha)_l - w(\alpha)_b)(b_{li} - b_{bi}).$$

Therefore, the gradient of the energy function in (9) is determined analytically and it can be easily used in gradient based minimization algorithms. To minimize the model (9), we apply the same approach as required by the Alg. 1, but in this case the model (7) is replaced by the regularized model (9).

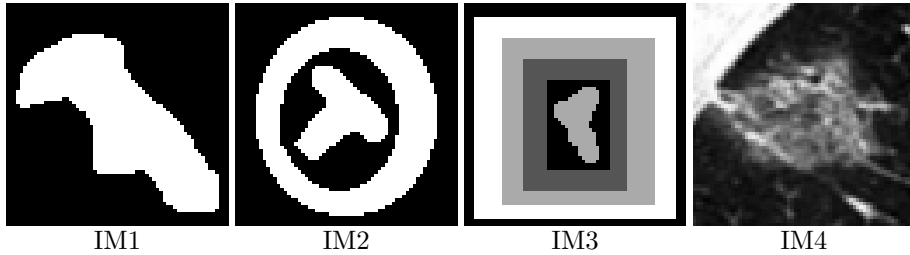


Fig. 4: Original test images used in experiments.

## 4 Experimental evaluation

In this Section a short experimental evaluation of the proposed NSST method is presented. Four test images are used in the experimental work, shown in Fig. 4. Images denoted by IM1 and IM2 are binary phantoms, while IM3 is a phantom with gray pixel intensities. Test image IM4 shows a fragment of a CT image of a human lung with stain caused by COVID-19 disease. All test images (64 x 64) have the same pixel intensity range of  $[0, 1]$ . These images are used as originals in the reconstruction experiments.

Table 1: Experimental results for IM1 and IM2 images, using three different reconstruction methods. The abbreviation  $d$  indicates the number of taken projection directions.

$d$	IM1				IM2				
	2	3	4	6	2	3	4	6	
NSST	$E_P$	2.22e-12	8.61e-08	6.44e-08	8.26e-08	1.73e-12	7.24e-08	8.63e-08	8.52e-08
	$E_R$	313.51	18.5770	5.30e-07	1.19e-06	1296	573.89	6.16	8.51e-07
	$rE_R$	23.93%	1.42%	$\approx 0\%$	$\approx 0\%$	78.83%	34.91%	0.37%	$\approx 0\%$
SPG	$E_P$	2.82	0	0	0	4.89	5.39	0	0
	$E_R$	21	0	0	0	1184	595	0	0
	$rE_R$	1.60%	0%	0%	0%	72.02%	36.19%	0%	0%
DC	$E_P$	23.49	6.91	6.69	7.87	23.49	17.96	16.50	10.65
	$E_R$	1325	27	12	10	1325	1007	236	30
	$rE_R$	1.01.15%	2.06%	0.92%	0.76%	80.60%	61.25%	14.36%	1.82%

The performance of the proposed NSST reconstruction method is compared with performances of three well-known reconstruction procedures: with the SPG [15, 14] and the DC [21, 22] algorithms for BT case, and with the SIRT [5, 20] algorithm for gray image reconstructions. All considered algorithms are implemented in Matlab environment.

The quality of the obtained reconstructions is expressed by the following three error measure functions

$$E_P(u^r) = \|Au^r - b\|,$$

$$E_R(u^r) = \sum_{i=1}^n |u_i^r - u_i^*|,$$

$$rE_R(u^r) = \frac{E_R(u^r)}{n_O} \cdot 100\%,$$

where  $u^r$  is the reconstructed image, while  $u^*$  denotes the original image and  $n_O$  is the number of object pixels in  $u^*$ . Function  $E_P$  is called *projection error* and its measures the accordance of the reconstruction with the given projection

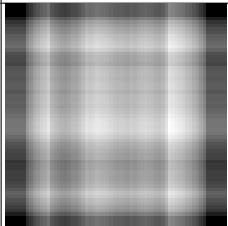
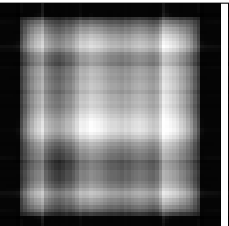
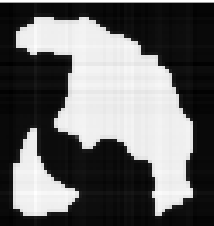
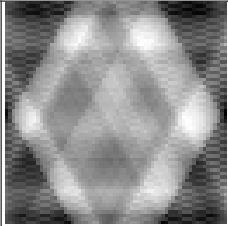
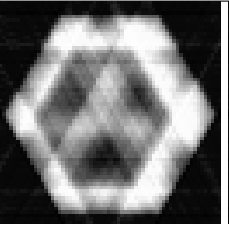

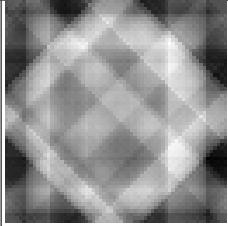
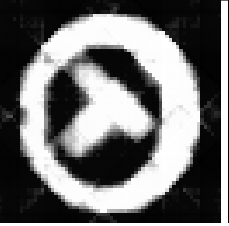

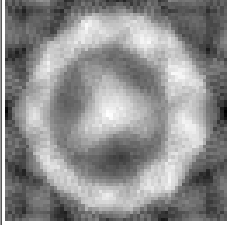
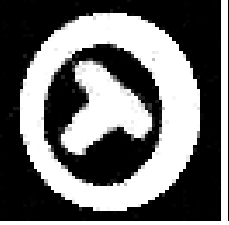

$d$	CG (least norm)	NSST (gray)	NSST (binary)
2			
	1438.88	1278.55	1296.20
3			
	1241.11	837.33	573.89
4			
	1198.80	265.31	6.16
6			
	823.19	58.20	8.51e-07

Fig. 5: Reconstructions of the phantom image IM2. The presented values below the reconstructions shows the corresponding reconstruction errors ( $E_R$ ).

data. The *reconstruction error*  $E_R$  expresses the distance of  $u^r$  from the original image  $u^*$ . In the case of binary reconstructions, the function  $E_R$  express the number of misclassified pixels, while  $rE_R$  express this number but relative to the size of the object, i.e., number of white pixels.

We note that the running time is not the advantage of the NSST method, mostly due to increased memory consumption and computational costs: the numerous  $(n - m)$  basis vectors  $\mathbf{b}_i \in \mathbb{R}^n$  of the null space of the projection matrix,

see Section 3, must be memorized and their linear combinations must be manipulated during the whole reconstruction process.

Table 1 shows the obtained reconstruction results for binary test images. The projection error  $E_P$  for NSST is close to zero in all experiments. If we round these values to zero, we can conclude that NSST performs the best regarding the projection error. In terms of the reconstruction error  $E_R$ , SPG is the winner in four cases, while in the remaining other four cases NSST gives the best results or shares first place with SPG.

Table 2: Experimental results for IM3 and IM4 images, using two different reconstruction methods. The abbreviation  $d$  indicates the number of taken projection directions.

$d$	IM3				IM4			
	10	15	20	25	10	15	20	25
$E_P$	8.71e-08	9.50e-08	9.78e-08	6.90e-08	9.42e-08	9.184e-08	8.85e-08	8.63e-08
NSST $E_R$	114.87	77.49	65.36	52.26	191.60	152.31	130.18	100.56
$E_P$	0.29	0.26	0.30	0.31	0.07	0.14	0.25	0.27
SIRT $E_R$	253.27	197.87	170.24	135.58	212.35	176.25	152.70	125.87

Table 2 summarises the obtained reconstructions results for gray test images. The NSST method has significantly better performance in all experiments, regarding both projection and reconstruction errors, than the "control" SIRT algorithm.

Fig. 5 shows three important phases of the proposed NSST reconstruction process for four different projection direction settings ( $d$ ). First column shows least norm reconstructions, obtained by the CG algorithm. In the next column we can see results of the second phase, where reconstructions are provided by the minimization model (3). The third column shows final results obtained by the regularized binarization model (9). We note, that the binarization process may be not "completed", which means that pixel intensities are not always purely binary, but just close to binary. The effect of this issue you can follow in cases of low amount of projection data, when  $d$  is 2 and 3. One of the possible reason for that can be the "highly" non convexity of the used potential function, see Fig. 3.

Fig. 6 shows reconstructions of gray images. NSST provides visually most appealing results in all presented cases.

Summarizing all obtained experimental results, we can conclude that that the proposed NSST method shows best performance regarding the projection error minimization, and also NSST shows good competence regarding the quality of reconstructions.

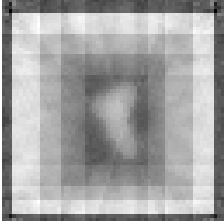
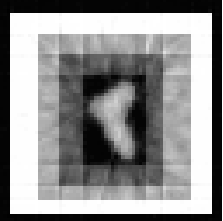


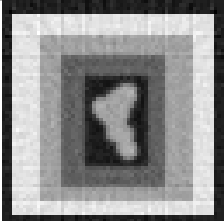
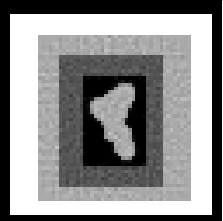

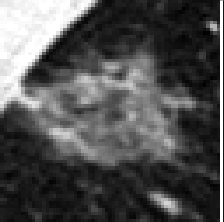
$d$	SIRT	NSST	SIRT	NSST
10				
	253.27	114.87	212.35	191.60
25				
	135.58	52.26	125.87	100.56

Fig. 6: Reconstructions of test images IM3 and IM4. The presented values below of reconstructions show the corresponding reconstruction errors ( $E_R$ ).

## 5 Conclusions

This paper introduces a new deterministic tomography reconstruction approach, called NSST. The proposed method is based on searching through linear combinations of the basis vectors of the null space of the projection matrix. One of the important advantages of the new method is that the projection error of the reconstruction guaranteed to remain at a minimum possible level, practically equal to zero. This is the case even when different regularization terms is involved into the reconstruction process. The minimization problem of the proposed reconstruction model is solved by a gradient based iterative algorithm. The obtained experimental results show good performance competence of the new method in comparison with three well-known reconstruction methods.

## Acknowledgement

Authors acknowledge the financial support of Department of Fundamental Sciences, Faculty of Technical Sciences, University of Novi Sad, in the frame of the Project "Primena opštih disciplina u tehničkim i informatičkim naukama". T. Lukić also acknowledges support received from the Hungarian Academy of Sciences through the DOMUS project.

## References

1. Batenburg, K.J., Sijbers, J.: Dart: A practical reconstruction algorithm for discrete tomography. *IEEE Transactions on Image Processing* **20** (2011)

2. Batenburg, K.J., Sijbers, J.: DART: A Fast Heuristic Algebraic Reconstruction Algorithm for Discrete Tomography. In: Proceedings of International Conference on Image Processing (ICIP). pp. 133–136 (2007)
3. Birgin, E., Martínez, J.: Spectral Conjugate Gradient Method for Unconstrained Optimization. *Appl. Math. Optimization* **43**, 117–128 (2001)
4. Carmignato, S., Dewulf, W., Leach, R.: *Industrial X-Ray Computed Tomography*. Springer (2018)
5. Gilbert, P.: Iterative methods for the three-dimensional reconstruction of an object from projections. *Journal of Theoretical Biology* **36**(1), 105–117 (1972). [https://doi.org/https://doi.org/10.1016/0022-5193\(72\)90180-4](https://doi.org/https://doi.org/10.1016/0022-5193(72)90180-4), <https://www.sciencedirect.com/science/article/pii/0022519372901804>
6. Gordon, R., Bender, R., Herman, G.T.: Algebraic reconstruction techniques (ART) for three-dimensional electron microscopy and x-ray photography. *Journal of Theoretical Biology* **29**(3), 471–481 (1970). [https://doi.org/https://doi.org/10.1016/0022-5193\(70\)90109-8](https://doi.org/https://doi.org/10.1016/0022-5193(70)90109-8), <https://www.sciencedirect.com/science/article/pii/0022519370901098>
7. Herman, G.T.: *Image reconstruction from Projections*. Springer-Verlag (1980)
8. Herman, G.T., Kuba, A.: *Discrete Tomography: Foundations, Algorithms and Applications*. Birkhäuser (1999)
9. Herman, G.T., Kuba, A.: *Advances in Discrete Tomography and Its Applications*. Birkhäuser (2007)
10. Herman, G.T., Kuba, A.: *Discrete tomography: Foundations, algorithms, and applications*. Springer Science & Business Media (2012)
11. Kisner, S.J.: *Image Reconstruction for X-Ray Computed Tomography in Security Screening Applications*. Ph.D. thesis, USA (2013)
12. Lukić, T.: *Discrete Tomography Reconstruction Based on the Multi-well Potential*. In: Proceedings of Combinatorial Image Analysis - 14th International Workshop (IWCIA). LNCS, vol. 6636, pp. 335–345. Springer-Verlag, Madrid, Spain (2011)
13. Lukić, T., Balázs, P.: Binary tomography reconstruction based on shape orientation. *Pattern Recognition Letters* **79**, 18–24 (2016)
14. Lukić, T., Balázs, P.: Limited-view binary tomography reconstruction assisted by shape centroid. *The Visual Computer (Springer)* **38**, 695–705 (2022)
15. Lukić, T., Lukity, A.: A Spectral Projected Gradient Optimization for Binary Tomography. In: *Computational Intelligence in Engineering, SCI*, vol. 313, pp. 263–272. Springer-Verlag (2010)
16. Lukić, T., Nagy, B.: Deterministic discrete tomography reconstruction method for images on triangular grid. *Pattern Recognition Letters* **49**, 11–16 (2014)
17. Lukić, T., Nagy, B.: Regularized binary tomography on the hexagonal grid. *Physica Scripta* **94**, 025201(9pp) (2019)
18. Lukić, T., Balázs, P.: Shape circularity assisted tomography reconstruction. *Physica Scripta* **95**(10), 105211 (sep 2020). <https://doi.org/10.1088/1402-4896/abb633>, <https://doi.org/10.1088/1402-4896/abb633>
19. Nocedal, J., Wright, S.J.: *Numerical Optimization*. Springer, New York, NY, USA, 2e edn. (2006)
20. Palenstijn, W.J., Bédorf, J., Sijbers, J., Batenburg, K.J.: A distributed astra toolbox. *Advanced Structural and Chemical Imaging* **2** (2016). <https://doi.org/10.1186/s40679-016-0032-z>
21. Schüle, T., Schnörr, C., Weber, S., Hornegger, J.: Discrete Tomography by Convex-concave Regularization and D.C. Programming. *Discrete Appl. Math.* **151**, 229–243 (2005)

22. Weber, S., Nagy, A., Schüle, T., Schnörr, C., Kuba, A.: A benchmark evaluation of large-scale optimization approaches to binary tomography. In: Proc. of 13th International Conference on Discrete Geometry for Computer Imagery (DGCI 2006). LNCS, vol. 4245, pp. 146–156. Springer-Verlag (2006)